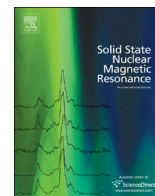




ELSEVIER

Contents lists available at ScienceDirect

Solid State Nuclear Magnetic Resonance

journal homepage: www.elsevier.com/locate/ssnmr

On the role of experimental imperfections in constructing ^1H spin diffusion NMR plots for domain size measurements



Ryan C. Nieuwendaal

National Institute of Standards and Technology, 100 Bureau Drive, Gaithersburg, MD 20899, United States

ARTICLE INFO

Article history:

Received 29 January 2016

Received in revised form

15 March 2016

Accepted 21 March 2016

Available online 24 March 2016

Keywords:

Solid-state NMR

CRAMPS

Domain size

Polymer blend

Composite

 ^1H spin diffusion

Miscibility

ABSTRACT

We discuss the precision of 1D chemical-shift-based ^1H spin diffusion NMR experiments as well as straightforward experimental protocols for reducing errors. The ^1H spin diffusion NMR experiments described herein are useful for samples that contain components with significant spectral overlap in the ^1H NMR spectrum and also for samples of small mass (< 1 mg). We show that even in samples that display little spectral contrast, domain sizes can be determined to a relatively high degree of certainty if common experimental variability is accounted for and known. In particular, one should (1) measure flip angles to high precision ($\approx \pm 1^\circ$ flip angle), (2) establish a metric for phase transients to ensure their repeatability, (3) establish a reliable spectral deconvolution procedure to ascertain the deconvolved spectra of the neat components in the composite or blend spin diffusion spectrum, and (4) when possible, perform 1D chemical-shift-based ^1H spin diffusion experiments with zero total integral to partially correct for errors and uncertainties if these requirements cannot fully be implemented. We show that minimizing the degree of phase transients is not a requirement for reliable domain size measurement, but their repeatability is essential, as is knowing their contribution to the spectral offset (i.e. the J_1 coefficient). When performing experiments with zero total integral in the spin diffusion NMR spectrum with carefully measured flip angles and known phase transient effects, the largest contribution to error arises from an uncertainty in the component lineshapes which can be as high as 7%. This uncertainty can be reduced considerably if the component lineshapes deconvolved from the composite or blend spin diffusion spectra adequately match previously acquired pure component spectra.

Published by Elsevier Inc.

1. Introduction

A straightforward, robust method for determining domain sizes and miscibility in two component polymer blends and pharmaceutical formulations is highly desired. One such approach is based on ^1H spin diffusion NMR, which has classically been utilized for degrees of mixing in blends [1–6], and continues to be a vital analytical tool for polymer blends [7,8], copolymers [9], pharmaceuticals [10], and dispersions [11]. Due to its high sensitivity, Combined Rotation And Multiple Pulse Spectroscopy (CRAMPS) [12] based ^1H spin diffusion is a fast method for determining degrees of miscibility. In CRAMPS experiments, strongly coupled spin systems like ^1H are modulated such that the homonuclear dipolar interactions are minimized during the multiple pulse cycle while other interactions (i.e. chemical shift) are left intact, though scaled. As a result, CRAMPS can yield ^1H NMR spectra with high signal-to-noise and chemical shift resolution of approximately 1 ppm or better. In chemically simple systems such as polymers, polymer

blends, and composites, this resolution is often sufficient and, when combined with ^1H spin diffusion methods, domain sizes in solid polymer blends can be determined.

In the seminal work by Clauss et al. [1], it was shown that domain sizes could be accurately determined via 2D chemical-shift-based (CSB) ^1H spin diffusion NMR when utilizing MREV-8 homonuclear decoupling [13]. This 2D CSB ^1H spin diffusion NMR experiment is a straightforward method for measuring domain sizes in blend samples that are not mass limited (10–100 mg) and when the two components do not overlap each other in the ^1H CRAMPS spectrum [1,8]. In this experiment, a 2D spectrum is collected for each spin-diffusion time investigated, which makes extensions of the technique to mass-limited samples (< 1 mg) difficult. We present here the 1D variant of that original experiment which uses a fixed number of MREV-8 cycles for preparation for each spin diffusion time chosen. This experiment has been utilized for determining domain sizes and miscibility of polymer blends [4–6] with applications in photoresists [14] and organic electronics [15] in which samples are typically mass-limited. While the 1D experiment has the drawback that it requires

E-mail address: ryann@nist.gov

additional background experiments for analysis, it has advantages in (1) shorter acquisition times and, hence, higher signal-to-noise ratios, so as to be applicable for measuring domain sizes in small samples (≈ 0.1 mg) such as thin films [16,17] and (2) samples in which the components exhibit extreme spectral overlap in the ^1H CRAMPS spectrum.

Domain sizes are extracted via spin diffusion NMR by measuring the rates of change of nuclear spin polarizations associated with the two phases in a blend or composite. When a step-function initial polarization gradient is imposed on a two-component system, the initial rate of exchange is directly proportional to the inter-component surface-area/volume ratio in the sample. From that ratio, the domain size can be extracted if the morphology is known (spheres, rods, lamellae) [18]. If the morphological character is not known, considerable error in the domain size can exist (factor of one to three) because similar curves could be predicted for different domain sizes depending on the morphological dimensionality [19]. Similarly, if the composition is not known (and cannot, for instance, be obtained via inspection of the ^1H spectrum), then additional error can exist since spin diffusion curves of blends with different compositions will differ even for similarly sized domains [19]. We will not comment on these errors in this paper because it is assumed that the sample morphology and/or composition can be ascertained via additional NMR measurements or another technique such as scattering or microscopy.

Due to the Fickian nature of spin flips, intra- and inter-monomer spin exchange occur simultaneously at early times of the spin diffusion process, which, depending on monomer size, is typically $< 1\text{--}3$ ms. At longer times, intra-monomer spin equilibration has been reached and inter-monomer spin exchange can unambiguously be monitored. In the 2D experiment, spin diffusion is measured from the build-up of cross-peaks between the two components' resonances on a 2D contour plot [1,8] and due to this greater spectral separation, *intra*-monomer spin exchange can, in principle, be distinguished from *inter*-monomer spin exchange. However, if ^1H chemical shift contrast is not sufficient, no spectrally isolated "cross-peak" would be identified on the contour plot, making it difficult to distinguish between intra- and inter-monomer spin exchange. In these cases either ^{13}C detection can be employed [20–23] which can require acquisition times that are orders of magnitude longer, or the spectra can be edited via addition/subtraction with the ^1H CRAMPS spectra of the components, necessitating background experiments.

The 1D experiment measures spin diffusion by monitoring the decay of the polarization of one of the components after a gradient has been established. In cases where both components in the blend contain aromatic and aliphatic resonances, there will be extreme spectral overlap in the ^1H spectrum and, similar to the 2D version, the feasibility of the experiment hinges on there being spectral isolation of one of the components somewhere in the spectrum. An example is given in Fig. 1, which shows the high resolution ^1H CRAMPS spectrum (Fig. 1a) of a blend of poly(3-hexylthiophene) (P3HT) and phenyl-C61-butyric acid methyl ester (PCBM) (50:50 by mass, 85:15 mol of ^1H). Also shown are spin diffusion spectra (Fig. 1(b)–(d)). The multiple pulse sequence is MREV-8 [13]. As shown in Fig. 1a, there is significant spectral overlap in the CRAMPS spectrum between P3HT (red) and PCBM (blue), but there is no appreciable spectral overlap at chemical shifts greater than 7.5 ppm. Despite severe spectral overlap from 1 ppm to 7.5 ppm, domain sizes could be ascertained from 1D ^1H CRAMPS spin diffusion by establishing, and then monitoring, the decay of the polarization gradient. The polarization gradient is realized by partially inverting the polarization of one of the components; in this case PCBM (Fig. 1b, blue) is inverted while

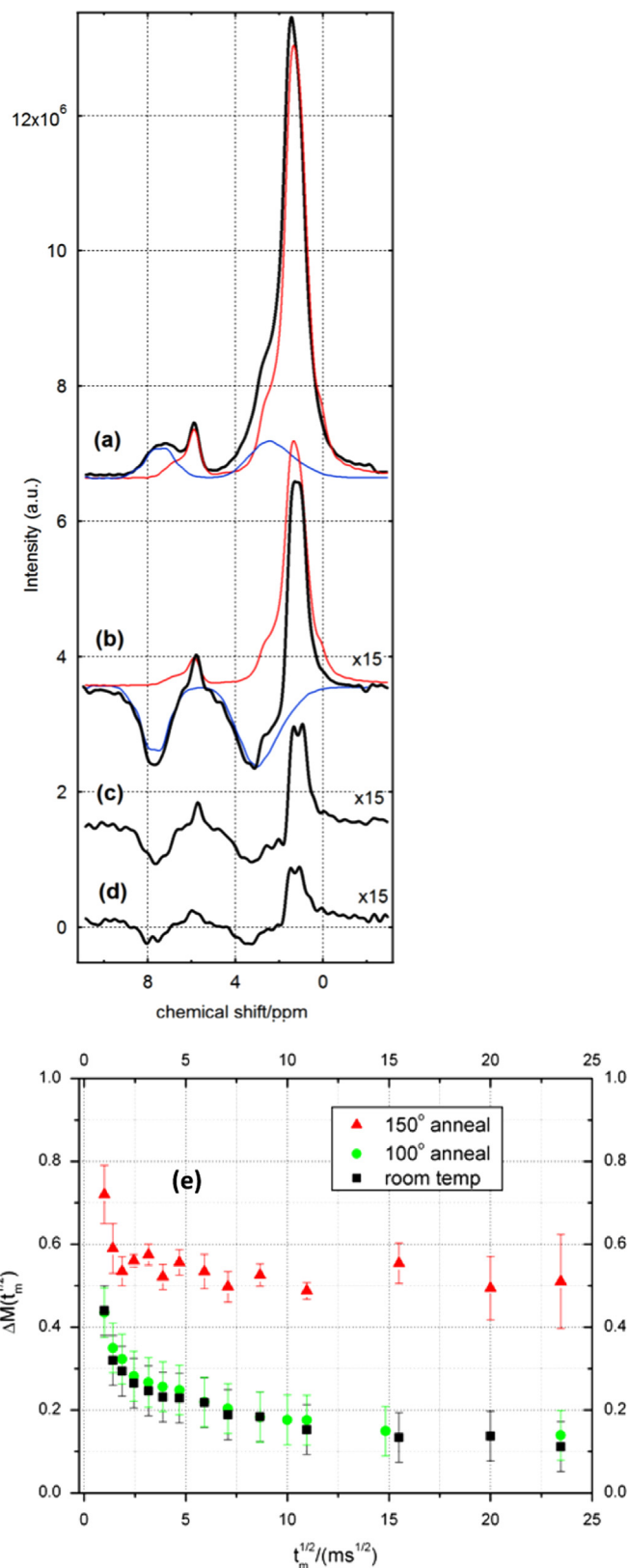


Fig. 1. (a) ^1H CRAMPS spectrum of a P3HT-PCBM blend (black) showing the individual components P3HT (red) and PCBM (blue), which were acquired separately. (b) ^1H spin diffusion spectrum at 2 ms mixing time (black) showing the individual components P3HT (red) and PCBM (blue), and mixing times of (c) 80 ms, and (d) 160 ms. (e) The spin diffusion plot of the P3HT-PCBM blend following different thermal annealing cycles. (For interpretation of the references to color in this figure legend, the reader is referred to the web version of this article.)

P3HT (red) has positive polarization. (The converse is not practical due to limitations in acceptable frequency offsets). The rate of decay is measured by monitoring the polarization of one of the components, $P(t)$, as a function of time; linear decays in polarization when plotted vs. the square root of time can directly be correlated to the domain size because of Fick's second law after accounting for T_1 relaxation effects.

The polarization is normalized via the equation:

$$\Delta M = \frac{P(t) - P(t=\infty)}{P(t=0) - P(t=\infty)} \quad (1)$$

where $P(t=\infty)$ is the polarization level at the infinite time limit, and $P(t=0)$ is the polarization level at the beginning of the mixing time. In blends in which the components' spectra overlap like this, one cannot know $P(t=0)$ directly from the sample's spin diffusion spectra since intra-monomer polarization gradients exist which can cause changes of intensity at early times. Conversely, since there can potentially be domains that are much larger than the longest spin diffusion radius ($\sqrt{4DT_1} < 200$ nm, $T_1 < 1$ s usually), the $P(t=\infty)$ value is not known either. These two polarization values are found by running a separate experiment on a composite that is coarsely grained (> 100 nm) by mechanical mixing (i.e. a "physical mixture") with identical chemical composition to the unknown blend sample so that the y -axis (ΔM) can be properly normalized via Eq. (1). As shown in Fig. 1e, when placed on a normalized spin diffusion plot the changes in domain sizes in a blend of P3HT and PCBM can be followed by monitoring the changes in the various plots. As shown from the relatively flat profile and larger intercept at longer times (Fig. 1e, red triangles), the 150 °C annealing of this particular sample caused dramatic coarsening because a portion of the PCBM was incorporated into large PCBM crystals ($> 1 \mu\text{m}$) [15].

As discussed above, the advantage of this particular experiment is that it can be successfully performed on systems that exhibit significant spectral overlap in the ^1H spectrum (i.e. both components contain aliphatic and aromatic protons) and in samples with low masses (< 1 mg). The disadvantage is that additional background experiments have to be performed on a physical mixture sample (and perhaps on the neat components, see below) for normalizing the spin diffusion plot. The focus of this paper is to identify the causes and potential limits of precision in measuring domain sizes via the spin diffusion plot as constructed from 1D ^1H spin diffusion NMR experiments. In particular, we discuss the effects of experimental limitations on the precision of establishing ΔM values which are critical for accurate and precise domain size determination. Since spin diffusion plots from 1D experiments on intimately mixed blends are normalized by comparing intensity levels to those of separate experiments on either a coarsely grained physical mixture sample or the neat components, determining the origin of experiment-to-experiment variability is critical for estimating precision and, ultimately, improving measurements. To determine the magnitude of these instrumental imperfections, we intentionally varied pulse amplitude (B_1), probe tuning (phase transients), sample morphology (lineshape), and frequency offset. We report the first three parameters as a function of frequency offset due to its convenience as a tunable parameter for establishing spin diffusion NMR experiments with zero total integral, which we will show below leads to higher precision.

2. Results/discussion

The cyclic nature of the multiple pulse decoupling in CRAMPS is responsible for minimizing the homonuclear dipolar coupling, but experimental imperfections slightly perturb the doubly rotating frame of observation (i.e. the toggling frame). Imperfections such as

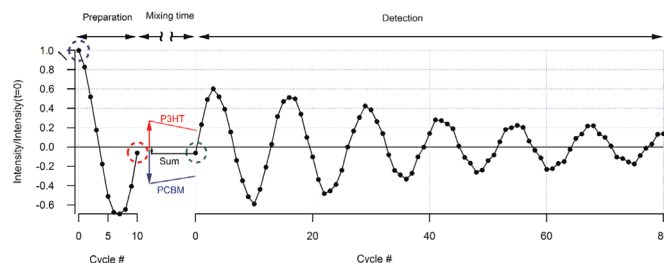


Fig. 2. Time domain profile of a 1D ^1H spin diffusion NMR experiment. After a fixed number of multiple pulse cycles in the preparation, some of the spins have inverted (PCBM, blue arrow) and some have not (P3HT, red arrow), also see Fig. 1b. The intensity in the red dotted circle, I_1 relative to the blue dotted circle, I_0 , is the weighted sum of both initial polarizations (see Eq. (2)). Spin diffusion between components will cause each polarization to decay during the mixing time (red "P3HT" line and blue "PCBM" line), but, in the absence of T_1 effects, the total intensity will not change (black "Sum" line). The polarizations are detected via CRAMPS after the mixing time and then Fourier transformed to obtain the "spin diffusion spectrum" (also see Fig. 1b–d). (For interpretation of the references to color in this figure legend, the reader is referred to the web version of this article.)

pulse amplitude (B_1) variability, phase offsets, and pulse rise/decay time effects ("phase transients," see below) all cause deviations from ideal CRAMPS behavior. The impacts of these imperfections were laid out over 40 years ago in the seminal paper on multiple pulse decoupling by Rhim and coworkers [24,25] and further expanded upon by Mehring [26]. Here, we utilize their formalism to demonstrate the sensitivity of these variables, which commonly occur in NMR, on 1D chemical-shift-based ^1H spin diffusion NMR experiments. Amplifier (B_1) drift, phase transients, and sample-to-sample variability all impact the reproducibility of the ^1H NMR chemical shift scale, which in turn, affects the frequency of oscillations in the spin diffusion preparation stage. Small deviations in frequency in the gradient preparation stage can significantly influence the polarization levels, and hence ΔM values, used for the spin diffusion plot for calculating domain sizes. Below we will show that, despite these polarization level deviations, they are *not* likely to lead to dramatic losses of precision in 1D ^1H spin diffusion NMR experiments if (1) polarization levels of known calibration standards (neat components and/or a physical mixture) are measured, (2) accurate values of B_1 are known, including susceptibility to drift, and (3) experiment-to-experiment variability of phase transients is minimized by way of direct measurement of tuning parameters such as the reflected voltage-to-forward voltage ratio, V_R/V_F . Furthermore, if these experimental conditions can be established, variations in ΔM values can be kept low ($< 7\%$), which ultimately will allow for domain sizes to be determined to high precision if the sample stoichiometry and morphological dimensionality are both known. Again, we quote no level of precision in domain size extracted here, only levels of precision of ΔM values, because the sensitivity of the domain size value to stoichiometry and sample morphology (i.e. spheres vs. lamellae) is so great (factor of 3 or greater).

In Fig. 2, we have plotted a typical time domain profile of a 1D ^1H spin diffusion NMR experiment. Our example is P3HT:PCBM. In the first stage (the preparation stage), the polarization gradient is created by allowing the magnetization to evolve under a fixed number of multiple pulse cycles, in this case ten. As shown in the blue circle, the intensity of the first data point, I_0 (the y -axis is scaled by I_0 for clarity), is identical to the total integrated intensity of the thermal equilibrium Fourier transformed CRAMPS spectrum (Fig. 1a) and is proportional to the proton magnetization, which is dictated by the Boltzmann distribution of spins. The intensity of the second data point (red dotted circle) is reflective of the magnetization after a fixed number of CRAMPS preparation cycles (i.e., ten). The magnetization then evolves during the mixing time, after which it is then detected via CRAMPS. The intensity of the first point in the detection period (third circled

data point from the left, green circle, Fig. 2), which we denote I , is equivalent to the total integral of the Fourier transformed spin diffusion spectrum (Fig. 1b). For a neat component, the ratio of these integrals, I/I_0 , is equivalent to the polarization relative to the thermal equilibrium polarization (Eq. (2a)). For a composite/blend of components A and B this ratio is a sum of the relative polarization values (Eq. (2b)) weighted by their proton mole fractions, ρ_A and ρ_B , respectively.

$$\left(\frac{I}{I_0}\right)_{A,B} = P_{A,B}(\text{individual A, B}) \quad (2a)$$

$$\left(\frac{I}{I_0}\right)_{\text{comp}} = \rho_A \cdot P_A + \rho_B \cdot P_B(\text{composite/blend}) \quad (2b)$$

In Fig. 2, the black line marked “Sum” is the weighted sum of the P3HT (red line) and PCBM (blue line). Furthermore, assuming negligible intensity loss due to longitudinal (i.e. T_1) proton relaxation, intensities of the second and third data points (in the red and green dotted circles) are essentially the same. Using Eqs. (2a) and (2b), one can use the following procedure for finding the polarization values in a blend needed for calculating ΔM , the y -axis of the spin diffusion plot (Eq. (1)). $P(t)$ is determined using the blend sample and $P(t=0)$ and $P(t=\infty)$ are obtained from the physical mixture. Since measurements of at least two samples, the “unknown” blend and the “standard” physical mixture, are needed in determining ΔM , it is critical to minimize variability in these measurements. If one seeks accurate ΔM values, how close to matching the experimental conditions does one have to be to ensure an identical polarization gradient is prepared in separate experiments?

What experimental variables affect the polarization gradient, and to what degree? Since a component's polarization is equal to the time domain intensity I (of that given component) relative to I_0 , the polarization gradient is clearly sensitive to the observed frequency under CRAMPS decoupling, which we denote by the oscillation in the preparation stage in Fig. 2. If the observed frequencies change as experimental parameters are altered, there will be a concomitant change in the polarization gradient. Fortunately, the sensitivity of MREV-8 decoupling to pulse width/amplitude offset, phase transients, phase errors, frequency offsets, rf inhomogeneity, and power droop have all been beautifully laid out [24–26]. In those previous works, the various contributions of errors to the rf Hamiltonian were separated and quantified by assuming the total rf Hamiltonian is the sum of an ideal, cyclic component and a non-ideal, non-cyclic component. The error factors of MREV-8 are given in Table 1.

Table 1

Contributions of various experimental errors to the Hamiltonian during MREV-8 decoupling. The variables are as follows: δ_i is pulse width/height misadjustment with phase i , l_i is the spin quantum number in the i th direction, J_1 is phase angle accumulated during a phase transient, t_c is the total cycle time (in this case 39.6 μ s), π_i is the phase offset of the pulse with phase i , $\Delta\omega$ is the angular frequency offset, ω_0 is the Larmor frequency, σ_{zzi} is the zz th component of the chemical shift tensor of the i th spin, a is the scaling factor of MREV-8 ($=\frac{3\omega_0}{t_c}(\frac{4}{\pi}-1)$), ω_s is the steady-state nutation frequency after power droop, b is the decay time of the power droop, and B_{ij} is the dipolar coupling constant between spins i and j . Higher order effects and cross-terms are not included.

Error	Correction term
Frequency offset	$\frac{1}{3} \sum_i (\Delta\omega + \omega_0 \sigma_{zzi}) (1 + 2a) (l_{xi} + l_{zi})$
Pulse width error	$\frac{2}{t_c} (-\delta_x + \delta_{-x}) l_x$
Phase transients	$\frac{2}{t_c} J_1 (l_x + l_z)$
Phase error	$\frac{2}{t_c} [(\phi_y - \phi_{-y}) l_x + (-\phi_{-x} + \phi_x) l_y]$
Power droop	$\frac{\omega_s t_w}{t_c} \frac{12}{b^2} e^{-\frac{12\pi}{b}} \sum_i \sum_{<j} B_{ij} [l_{yi} (l_{xj} + l_{zj}) + (l_{xi} + l_{zi}) l_{yj}]$

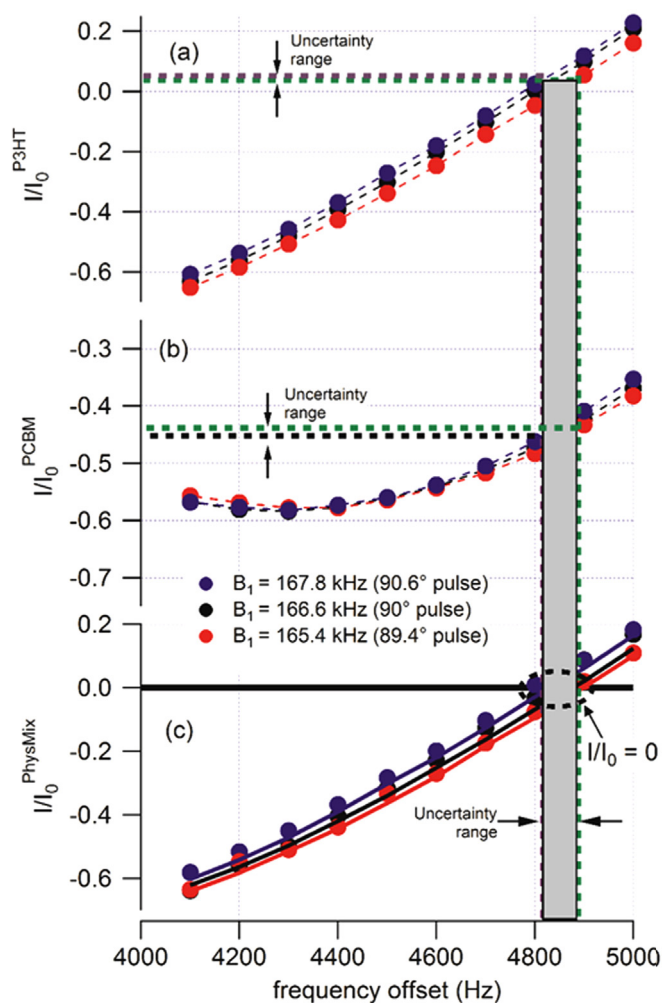


Fig. 3. Integral of the spin diffusion spectrum (I) relative to the CRAMPS spectrum (I_0) recorded after 3 ms mixing time for samples of (a) P3HT, (b) PCBM, and (c) their physical mixture for slight increases (blue) and decreases (red) in B_1 as a function of frequency offset. The thin dotted lines between points in (a) and (b) are a guide for the eye. The thick lines in (c) are calculated from Eq. (2b) with $\rho_{PCBM} = 0.15$ and $\rho_{P3HT} = 0.85$. (For interpretation of the references to color in this figure legend, the reader is referred to the web version of this article.)

2.1. Effect of pulse amplitude on I/I_0 uncertainty

We measured I/I_0 on individual samples of P3HT and PCBM as well as their physical mixture. In the case of neat materials (P3HT and PCBM), the polarization level, which is constrained to be within the range from -1 to 1 , is calculated via the integrated intensity, I , in a spin diffusion experiment relative to the CRAMPS spectrum intensity, I_0 . We note again that this ratio is identical to the intensity of the $(n+1)$ st data point in the preparation period (Fig. 2, red circle) relative to the first data point (Fig. 2, blue circle), where n is the number of preparation cycles. In Fig. 3, we plot I/I_0 as a function of offset frequency for (a) P3HT, (b) PCBM, and (c) their physical mixture (50:50 by mass). The mixing time is fixed at 3 ms, and the range of acceptable carrier frequency offsets (3500–5000 Hz) is limited by the effectiveness of CRAMPS (offset < 5000 Hz) and avoided overlap with the spectrum (offset > 3500 Hz). As shown in the figure, even for small drifts in pulse amplitude of approximately 1.4 kHz, which correspond to $\pm 0.6^\circ$ flip angle offsets, δ_x , (see Table 1, second row), significant polarization variability can be observed of up to ± 0.04 . In the case of a 50:50 blend of P3HT with a typical PCBM polarization $P_{PCBM} = -0.44$, this would correspond to an uncertainty spread in ΔM of

18% (=0.08/0.44), clouding any meaningful analysis.

Clearly the potential exists for greater precision to be garnered from a ^1H spin diffusion plot. To do so, the same I/I_0 value must be maintained in both the physical mixture and the blend sample; this is done by intentionally changing the frequency offset until $I/I_0=0$. Improvements in sensitivity in NMR exchange experiments when intentionally setting a zero-integral initial condition have been previously reported. [27] When looking at the plot of the physical mixture (Fig. 3c), one observes that (like Fig. 3a and b) the I/I_0 values change with frequency offset and that different curves are observed for different B_1 values (black, red, and blue dots). The black dots correspond to I/I_0 values in which the B_1 field was precisely known to be 166.6 kHz; the blue and red dots correspond to B_1 values that were intentionally mis-set by 1.2 kHz too high and too low, respectively. If the experiment is conducted while keeping $I/I_0=0$ (see the dotted black circle in Fig. 3c), then drifts in the B_1 value by ± 1.2 kHz would result in a range or band of frequency offset values that would satisfy $I/I_0=0$ (Fig. 3, gray box). This range of frequency values lies within the purple (frequency offset = 4810 Hz) and green (frequency offset = 4880 Hz) vertical dotted lines in Fig. 3 and these positions represent the *extremes* of error in CRAMPS frequency due to B_1 drift for the spectrometer in our laboratory. The polarization values for the two components that would be observed with these CRAMPS frequencies can be known by following the vertical dotted lines (purple and black) up into Fig. 3a, b and monitoring at what I/I_0 values the lines intersect. The polarization values (y -axes, I/I_0) at these conditions (horizontal dotted lines) represent the extrema of the uncertainty ranges, which upon inspection of Fig. 3a and b, are relatively narrow ($< 1\%$), translating in a spread of ΔM values of $< 2\%$. Hence, one sees that although a spread in B_1 values might cause a spread in CRAMPS frequencies, the impact on uncertainty or spread in the polarization levels for spin diffusion experiments performed when maintaining $I/I_0=0$ is low.

To further test the reliability and repeatability, we have synthesized what the physical mixture I/I_0 values should be (solid lines through the data, Fig. 3c) based on the known polarization levels of the neat components (Fig. 3a and b) and the proton fractions ($\rho_{P3HT}=0.85$, $\rho_{PCBM}=0.15$) using Eqs. (2a) and (2b). As one can see, the agreement with experiment and prediction is quite good. The two caveats are that (1) agreement exists between the deconvolved physical mixture lineshapes and neat component lineshapes, and (2) the rf probe tuning is consistent. We next explore the impact of uncertainty in those two parameters.

2.2. Effect of phase transients on polarization level uncertainty

Each NMR probe suffers from ring down effects because of its inherent RLC time constant or quality factor (Q factor). CRAMPS experiments use cycles of phase sensitive pulses for decoupling, and the rise/decay times of these pulses create non-ideal fields which are non-linear and out-of-phase with the peak of the pulse; these perturbations are called “phase transients” [28,29] and schemes for reducing their effects have been outlined [30]. Phase transients will cause a frequency shift in the observed CRAMPS spectrum, but will not result in spectral broadening [24–26]. Tuning the probe effects the Q factor directly, and consequently any variability in tuning will result in a frequency shifts under multiple pulse decoupling.

In Fig. 4 we have plotted the magnitude of the observed CRAMPS resonance frequency offset for the narrow resonance of the methyl protons of poly(di-methyl-sulfoxide) (PDMS) as a function of carrier frequency offset for different tuning levels. A clear shift in the observed frequency occurs upon changing the tuning. This is expected since tuning the probe would alter the rise/fall times of the pulses and, hence, the J_1 coefficient (Table 1,

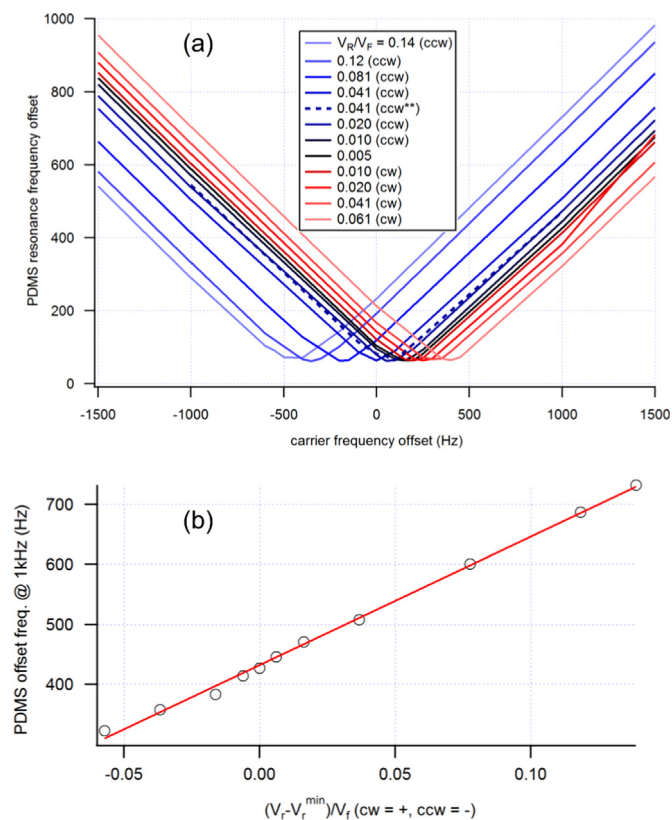


Fig. 4. (a) The *absolute value* of the observed resonance frequency offset of PDMS (non-quadrature, cosine detection) as a function of the carrier frequency offset for different reflected voltage-to-forward voltage ratios (V_R/V_F) by changing the tuning capacitor clockwise (cw) or counterclockwise (ccw). Changes in the matching capacitor showed similar behavior as long as the V_R remained constant (see the blue dotted line as an example). (b) The observed frequency offset of PDMS with a 1000 Hz carrier frequency offset as a function of V_R/V_F difference from the minimum value; $V_R^{\min} = (40 \pm 10)$ mV and $V_F = 9.8$ V. For convention, we denote negative V_R values as clockwise turns of the tuning capacitor and positive as counterclockwise. The values of the best fit line (red curve) to $y = m \cdot x + b$ are $m = (2141 \pm 37)$ Hz, $b = (432 \pm 2)$ Hz. (For interpretation of the references to color in this figure legend, the reader is referred to the web version of this article.)

third row). The frequency offset and phase transient correction terms (Table 1, rows 1 and 3, respectively) both contain I_z terms, and should add linearly. Hence, when plotting the observed frequency offset vs. carrier frequency offset as in Fig. 4, the curves should be linear with the slope equal to the scaling factor and with an ordinate equal to $\frac{2J_1}{2\pi c}$. However, no curves pass through the origin; the minimum CRAMPS frequency is at ≈ 65 Hz, demonstrating that phase transient effects persist for all tuning configurations, in violation of the first order effects mentioned here. We attribute the persistence of phase transient effects and the curves not passing through the origin to higher order and/or cross-term effects as discussed in Ref. [24]. Importantly, as we show below, the persistence of phase transients does little to effect the precision with which ΔM values can be calculated if the sensitivity of the frequency change to the tuning is predictable (see Fig. 4b below).

For a given carrier frequency (in this case 1 kHz), the observed CRAMPS frequency will change linearly with the reflected voltage level via the empirical equation:

$$v = (2141 \text{ Hz}) \cdot \left(\frac{V_r - V_r^{\min}}{V_f} \right) + 432 \text{ Hz} \quad (3)$$

Furthermore, when the receiver is in phase with the signal, the polarization is a cosine function and any changes in polarization go as:

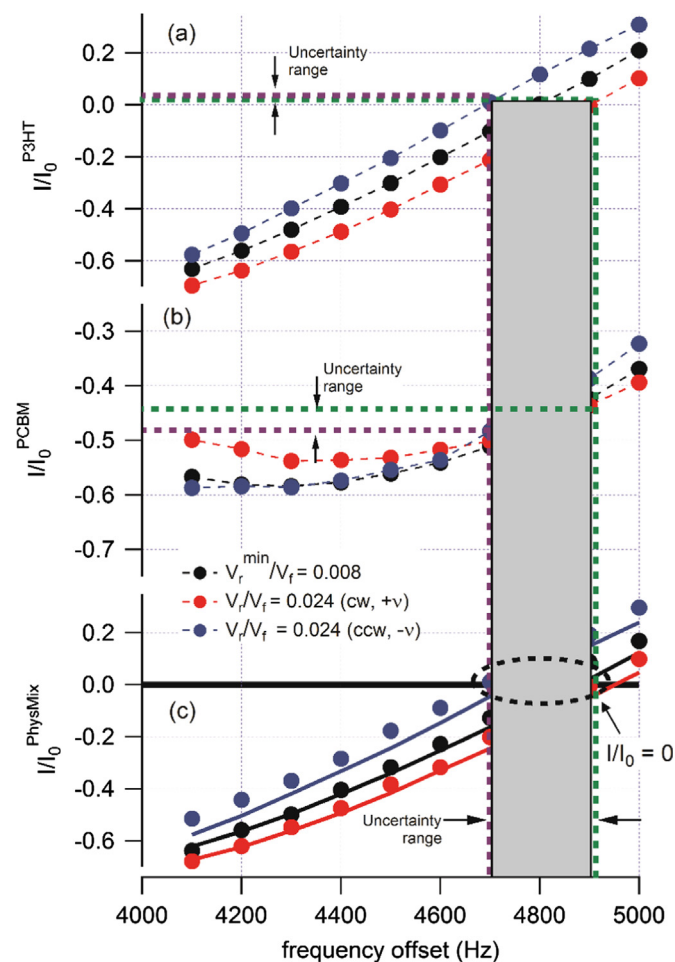


Fig. 5. Integral, I , of the spin diffusion spectrum (10-cycle CRAMPS preparation) relative to the equilibrium CRAMPS spectrum (I_0) as a function of frequency offset for P3HT (a), PCBM (b), and their physical mixture (c) for different V_R/V_F values as observed upon changing the tuning capacitor cw (red dots) and ccw (blue dots). The forward voltage was measured to be 4.1 V. Spectra were recorded after 3 ms mixing time. (c) The solid lines are calculated from the values in (a) and (b) using Eq. (2b). (For interpretation of the references to color in this figure legend, the reader is referred to the web version of this article.)

$$\frac{dP}{d\nu} = -2\pi t \cdot \sin(2\pi\nu_{obs}t). \quad (4)$$

Since P is simply a cosine function assuming negligible damping. Here, ν_{obs} is the observed CRAMPS frequency offset (Fig. 4a, y-axis), which is a function of carrier frequency offset and tuning (see Fig. 4a, x-axis); t is the total preparation time, which in these experiments is 0.396 ms. The maximum expected rate of change in polarization is the coefficient $-2\pi t$, which is -0.0029 in units of polarization/Hz. Combining this value with Eq. (3) yields a maximum change in polarization upon changes in tuning to be 6.2 (units of polarization per unit of V_R/V_F). Typical (normalized) variations in tuning are less than 0.02 (see below), translating into changes of polarization of less than 0.1.

We have plotted the I/I_0 values of P3HT (a), PCBM (b), and their physical mixture (c) as a function of frequency offset in Fig. 5 for three tuning levels. The black dots, which correspond to the lowest V_R/V_F value ($0.04/4.9=0.008$) and hence “best” tuning scenario, are shown for P3HT (Fig. 5a), PCBM (Fig. 5b), and the physical mixture (Fig. 5c). The blue and red dots in Fig. 5 are polarizations measured upon detuning the tuning capacitor clockwise and counterclockwise, respectively, to attain $V_R/V_F=0.024$. In the case of P3HT (Fig. 5a), the polarization levels change significantly (*ca.* ± 0.1) depending on the tuning capacitor direction; this value is as predicted from via Eq. (4) for $(\frac{V_r - V_r^{min}}{V_f})=0.016$, $t=0.396$ ms, and $\nu_{obs} \approx 2.1$ kHz (at 4800 Hz).

The I/I_0 changes for PCBM (Fig. 5b) are less dramatic because the higher fraction of aromatic protons (0.36:0.64 aromatic:aliphatic protons) moves the observed offset frequency to lower ν_{obs} values (≈ 1520 Hz at a carrier frequency offset of 4800 Hz), decreasing the $\frac{dP}{d\nu}$ quantity. Note that at a frequency offset of *ca.* 4700 Hz, there is essentially no change in the PCBM polarization level with detuning; this is due to the fact that $2\pi\nu_{obs}t \approx 0$.

The precision of determining ΔM values on the spin diffusion plot ultimately depends on the variability of the polarization levels at $I/I_0=0$ (black dotted circle, Fig. 5c). If the $(\frac{V_r - V_r^{min}}{V_f})$ values changed on the order of ± 0.024 from one experiment to the next, then in order to maintain $I/I_0=0$, a spread of possible frequency offsets would be required (Fig. 5, gray box) in order to maintain $I/I_0=0$ that ranged from 4700 Hz (Fig. 5, purple dotted line) to 4920 Hz (Fig. 5, green dotted line). We use these tuning conditions as extremes of drift; one can typically maintain V_R values to within a factor of 0.2, not 3. At these extremes, the I/I_0 values for PCBM range from -0.43 to -0.48 (Fig. 5b, horizontal purple/green lines); those of P3HT range from 0.01 to 0.02 (Fig. 5a, horizontal purple/green lines). When using P_{PCBM} to calculate ΔM from Eq. (1) (because of its greater spectral isolation at chemical shifts > 7.5 ppm, see Fig. 1a), then the observed spread in polarization levels (± 0.025) translates into a spread of ΔM values of ± 0.028 if the probe tuning (as measured via the V_R/V_F) is not known to within a factor of three. The V_R/V_F value is typically known to with a factor of 0.2 (not 3) and will allow for greater predictability. For instance, the solid lines in Fig. 5c are I/I_0 values as predicted from a linear combination of the neat component I/I_0 values (Fig. 5a and b) using Eqs. (2a) and (2b); the agreement is good.

2.3. Sample-to-sample variability

When performing experiments with $I/I_0=0$ in the physical mixture or blend, a third source of precision loss comes from variations in the spectra. Changes in the resonance positions can occur as a result of variations in magnetic susceptibility anisotropy, molecular packing, and molecular conformations. We tested this variability by making ordered and disordered samples of P3HT and PCBM. We assume similar spin diffusion coefficients between ordered and disordered samples because we have generally observed similar T_2 values amongst sample sets and T_2 times are used to calculate spin diffusion coefficients [1]. We have plotted in Fig. 6 the CRAMPS spectra for P3HT (a), PCBM (b), and the physical mixture (c) for both ordered and glassy samples. There are subtle differences in linewidths between the various samples depending on order, in particular the PCBM samples, in which the glassier sample exhibits essentially no fine structure (Fig. 6b, red spectrum), but the ordered PCBM does (Fig. 6b, black spectrum).

These spectral changes translate into changes for the spin diffusion experimental conditions. As shown in Fig. 6(d)–(f), the I/I_0 vs. frequency offset curves depend on whether the sample was ordered (black dots) or glassy (red dots) and result in a band of possible offset frequency values for which $I/I_0=0$ in the blend (Fig. 6(c)–(e), gray box). For the ordered physical mixture, $I/I_0=0$ at 4900 Hz (Fig. 6, vertical green dotted line); for the glassy sample $I/I_0=0$ at 4780 Hz (Fig. 6e, vertical purple dotted line). This spread of conditions translates into an uncertainty of the P3HT I/I_0 values of 0.07 to 0.1 (Fig. 6d, purple and green horizontal lines, respectively). For PCBM, the spread of I/I_0 values range from -0.42 to -0.39 (Fig. 6e, horizontal purple and green dotted lines) depending on order. If the PCBM polarization values are used to construct the spin diffusion plot using Eq. (1), then, based on the spread in those values, one would expect a spread of ΔM values of approximately 0.07.

With spectral deconvolution, error can potentially be reduced if 1) one can reliably synthesize (via spectral differences) artifact-free, adequately phased spectra of the neat components from the

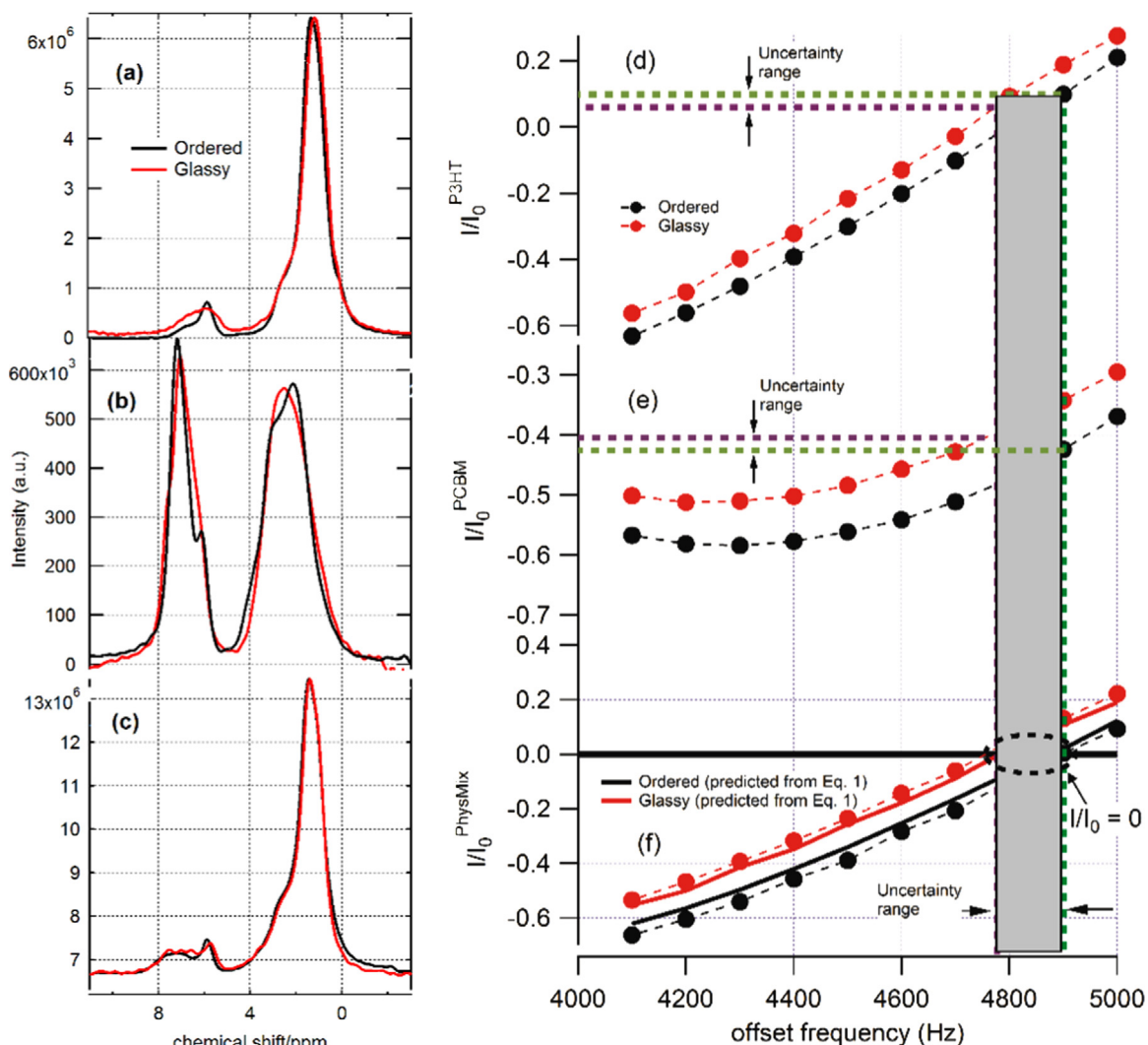


Fig. 6. CRAMPS spectra of (a) P3HT, (b) PCBM, and (c) physical mixtures of P3HT and PCBM. Samples were either ordered (black) or disordered (red). (d)–(f) Plots of polarization vs. frequency offset for P3HT (d), PCBM (e), and physical mixture of P3HT and PCBM (f) for either ordered (black) or glassy (red) samples. (For interpretation of the references to color in this figure legend, the reader is referred to the web version of this article.)

composite CRAMPS spectrum and 2) there are negligible differences between the deconvolved spectra and those of previously acquired spectra of the neat components. In our lab, we have generally found this to be feasible, particularly if spin diffusion spectra are acquired together with CRAMPS spectra via block averaging to minimize drift on short time scales ($<$ minutes). In practice, one could qualitatively check the extent to which the spectral features resemble either previously run samples, and use the most appropriate I/I_0 value (i.e. “ordered” or “disordered”) to calculate ΔM . This procedure will result in a much more precise ΔM . For instance, since we knew the lineshapes of the ordered and glassy samples and their polarizations, we were able to easily predict the I/I_0 values in the physical mixture (Fig. 6e, solid lines) with a high degree of certainty as witnessed by the agreement of the experimental data (black/red dots, Fig. 6e). However, if the experimental spectrum does not resemble either synthesized single component spectrum, an estimate of the applicable I/I_0 value *could* be obtained (but as of yet untested in our lab) by the inverse Fourier transform of the synthesized spectrum to obtain the time-domain data, in which the ratio of the $(n+1)$ st data point to the first data point would yield the proper I/I_0 value. One potential issue preventing a precise I/I_0 estimate using this method

would be from artifacts arising from baseline and phasing issues, which could perturb the intensity of the first time domain point.

3. Conclusions

Despite significant spectral overlap in the ^1H CRAMPS spectrum, with straightforward experimental protocols, errors can be significantly reduced to $< 1\%$ in ^1H CRAMPS-based spin diffusion NMR measurements depending on the sample. Domain sizes can be determined to relatively high degree of certainty if a morphology dimensionality is known, flip angles are known to high precision ($\approx \pm 1^\circ$), the reflected voltage-to-forward voltage is known and reproducible, the blend spectrum can be deconvolved into the neat-component spectra, and experiments are performed close to zero-total integral where corresponding spectra are adjusted, using the equilibrium lineshape, to the zero-integral condition before analysis. Criteria b through d relate mainly to the establishment of the proper scaling for the ΔM plots, or, equivalently, to the correct determination of the initial average-polarization gradient between the two components. If the component spectra that are deconvolved in the blend sample do not adequately match those of previously acquired neat component

spectra, the largest contribution to error can be as high as $\approx 7\%$.

4. Experimental

4.1. Materials

P3HT (Plexcore 2100, Plextronics Inc., Pittsburgh, PA) and PCBM (99.5%, NanoC Inc., Westwood, MA) were used as received. According to the manufacturer the P3HT is ultra-high purity (< 25 ppm trace metals) and highly regioregular ($> 98\%$ head-to-tail), with a number averaged molar mass of 64500 g/mol and polydispersity index (PDI) of ≤ 2.5 . Ordered films were prepared by drop casting solutions (15 mg/mL) in chlorobenzene into a Teflon-well plate; films formed in approximately (4–6) h. Glassy films were prepared by drop casting solutions (15 mg/mL) in chloroform ($> 99.8\%$) onto a 70 °C heated Teflon substrate; films formed in < 5 s. The samples were ≈ 5 mg. The chloroform ($> 99.8\%$) and chlorobenzene ($> 99.8\%$) were used as received. P3HT films were sliced into approximately fifty fine flakes of ≈ 0.1 mm dimension and (lightly) pressed into disks to ensure isotropy and homogeneity in the NMR experiments. PCBM powder was collected with a non-magnetic stainless steel spatula. The P3HT/PCBM blend sample (Fig. 1) was drop cast into a chlorobenzene Teflon-well plate, removed with a non-magnetic stainless steel spatula and, if applicable, thermally annealed on a hot plate at 150 °C in a glovebox for 30 min. Additional characterization of the blend samples are given in [15].

4.2. NMR characterization

CRAMPS NMR experiments were performed on Bruker DMX300 spectrometer (7.05 T) at 300.13 MHz, a 5 mm Doty CRAMPS probe, and with the MREV-8 pulse sequence [3] with the following parameters: eight 1.5 μs $\pi/2$ pulses, cycle time 39.6 μs , 400 data points, 8–32 scans, 8 s recycle delay and 65136 zero filling points. Silicon nitride rotors with Kel-F caps and spacers were used for magic angle spinning.

This work was carried out by the National Institute of Standards and Technology (NIST), an agency of the U.S. government, and by statute is not subject to copyright in the United States. Certain commercial equipment, instruments, materials, services, or companies are identified in this paper in order to specify adequately the experimental procedure. This in no way implies endorsement or recommendation by NIST.

Acknowledgment

M.P. Donohue, V.M. Prabhu, D.L. VanderHart, and C.L. Soles are acknowledged for their thoughtful comments and edits of this manuscript.

References

- [1] J. Clauss, K. Schmidt-Rohr, H.W. Spiess, *Acta Polym.* 44 (1993) 1–17.
- [2] S. Spiegel, K. Landfester, Lieser, C. Boeffel, H.W. Spiess, M. Eidam, *Macromol. Chem. Phys.* 196 (1995) 985–993.
- [3] S. Li, D.M. Rice, F.E. Karasz, *Macromolecules* 27 (1994) 2211–2218.
- [4] G.C. Campbell, D.L. VanderHart, *J. Magn. Reson.* 96 (1992) 69.
- [5] D.L. VanderHart, G.C. Campbell, R.M. Briber, *Macromolecules* 25 (1992) 4734–4743.
- [6] D.L. VanderHart, J.D. Barnes, R. St John Manley, *Macromolecules* 27 (1994) 2826.
- [7] K. Schaler, M. Roos, P. Micke, Y. Golitsyn, A. Seidlitz, T. Thurn-Albrecht, H. Schmeider, G. Hempel, K. Saalwächter, *Solid State Nucl. Magn. Reson.* 72 (2015) 50–63.
- [8] W. Fu, R. Zhang, B. Li, L. Chen, *Polymer* 54 (2013) 472–479.
- [9] A. Fernandez, M.T. Exposito, B. Pena, R. Berger, J. Shu, R. Graf, H.W. Spiess, R. A. Garcia-Munoz, *Polymer* 61 (2015) 87–98.
- [10] J. Schlagnitweit, M.X. Tang, M. Baías, S. Richardson, S. Schantz, L. Emsley, *J. Magn. Reson.* 261 (2015) 43–48.
- [11] M.V. Mokeev, V.V. Zuev, *Eur. Polym. J.* 71 (2015) 372–379.
- [12] L.M. Ryan, R.E. Taylor, A.J. Paff, B.C.J. Gerstein, *J. Chem. Phys.* 72 (1980) 508.
- [13] W.K. Rhim, D.D. Elleman, R.W. Vaughan, *J. Chem. Phys.* 58 (1973) 1772–1773.
- [14] D.L. VanderHart, V.M. Prabhu, E.K. Lin, *Chem. Mater.* 16 (2004) 3074–3084.
- [15] R.C. Nieuwendaal, C.S. Snyder, R.J. Kline, E.K. Lin, D.L. VanderHart, D. M. DeLongchamp, *Chem. Mater.* 22 (2010) 2930–2936.
- [16] D.L. VanderHart, V.M. Prabhu, K.A. Lavery, C.L. Dennis, A.B. Rao, E.K. Lin, *J. Magn. Reson.* 201 (2009) 100–110.
- [17] R.C. Nieuwendaal, H.W. Ro, D.S. Germack, R.J. Kline, M.F. Toney, C.K. Chan, A. Agrawal, D. Gundlach, D.L. VanderHart, D.M. DeLongchamp, *Adv. Funct. Mater.* 22 (2012) 1255–1266.
- [18] K. Schmidt-Rohr, H.W. Spiess, *Multidimensional Solid State NMR and Polymers*, Academic Press, London, 1994.
- [19] D.L. VanderHart, G.B. McFadden, *Solid State Nucl. Magn. Reson.* 7 (1996) 45–66.
- [20] X. Jia, X. Wang, A.E. Tonelli, J.L. White, *Macromolecules* 38 (2005) 2775–2780.
- [21] J. Jia, X. Wolak, Wang, J.L. White, *Macromolecules* 36 (2003) 712–718.
- [22] J. Mao, X. Cao, *Limnol. Oceanogr.: Methods* 9 (2011) 533–542.
- [23] A. Rawal, X.Q. Kong, Y. Meng, J.U. Otaigbe, K. Schmidt-Rohr, *Macromolecules* 44 (2011) 8100–8105.
- [24] W.K. Rhim, D.D. Elleman, L.B. Schreiber, R.W. Vaughan, *J. Chem. Phys.* 60 (1974) 4595–4604.
- [25] M. Mehring, J.S. Waugh, *Phys. Rev. B* 5 (1972) 3459–3471.
- [26] M. Mehring, *Principles of High Resolution NMR in Solids*, Chap. 3, Multiple Pulse NMR Experiments, 2nd Ed., Springer-Verlag, Berlin, pp. 63–128.
- [27] N.M. Szeverenyi, A. Bax, G.E. Maciel, *J. Am. Chem. Soc.* 105 (1983) 2579–2582.
- [28] M. Mehring, J.S. Waugh, *Rev. Sci. Instr.* 43 (1972) 649–653.
- [29] T.M. Barbara, J.F. Martin, J.G. Wurl, *J. Magn. Reson.* 93 (1991) 497–508.
- [30] D.P. Burum, M. Under, R.R. Ernst, *J. Magn. Reson.* 43 (1981) 463–471.